Short Communication

Synthesis and Electrochemical Properties of Er^{3+} Doped Li[Li$_{0.2}$Mn$_{0.54}$Ni$_{0.13}$Co$_{0.13}$]O$_2$ as Cathode Materials for Lithium Ion Bateries

Wang Shicheng[*], *Ji Ling, Tang Xiaowen*

School of Economics and Management Beijing University of Technology, 100124 Beijing, China
[*]E-mail: shicheng@bjut.edu.cn

Li$_{1.20}$[Mn$_{0.54}$Ni$_{0.13}$Co$_{0.13}$]$_{0.80-x}$Er$_x$O$_2$ (x = 0, 0.01, 0.02, 0.03) cathode materials were synthesized using a combination of co-precipitation and high-temperature sintering. XRD, SEM, and TEM analyses and galvanostatic charge-discharge tests were carried out to study the influences of Er^{3+} doping on the crystal structural, morphology and electrochemical properties of Li$_{1.20}$Mn$_{0.54}$Ni$_{0.13}$Co$_{0.13}$O$_2$. The XRD results revealed that Er^{3+} doping decreased the cation mixing degree. The galvanostatic charge-discharge test results showed that improved electrochemical properties were obtained through Er^{3+} doping. With an increasing Er^{3+} doping content, the capacity retentions were enhanced from 88.1% to 92.8% and then decreased to 90.2% after 100 cycles with x = 0.01, 0.02 and 0.03, respectively, while the undoped sample delivered a capacity retention of 84.6%. In addition, the discharge capacity of Li$_{1.20[}$Mn$_{0.52}$Ni$_{0.13}$Co$_{0.13}$Er$_{0.02}$]O$_2$ was approximately 23.0 mAh g^{-1} larger than that of the undoped sample at a high rate of 5 C.

1. INTRODUCTION

With the rapid development of electric vehicles and hybrid electric vehicles, high demands for the energy density of lithium ion batteries continually increase[1,2]. Solid solutions composed of laminar Li$_2$MnO$_3$ and LiMO$_2$ (i.e., xLi$_2$MnO$_3$·(1-x)LiMO$_2$ (M = Mn, Ni, Co, etc.)) have aroused great interest from scholars due to its discharge capacity above 250 mAh g^{-1}. However, from the intensive studies, it has been found that there exist some defects in cathode materials, mainly resulting in great loss of the initial irreversible capacity, poor discharge performance at high rates and severe attenuation of the cycling performance, etc. Aimed at handling the defects, various methods (e.g., ion doping,

surface coating, surface acid treatment and heat treatment) have been adopted to refine the comprehensive electrochemical properties[5-8]. Particularly, as one of the most competitive modification methods, ion doping modification is a simple processing technique and performs excellently in synthesis [9,10]. During battery cycling, ion doping modification can maintain the structural stability of cathode materials through abating cation mixing. In the interior of the batteries, the existence of trace water can decompose into HF. Since the classical doping elements (e.g., Fe^{3+}[11] and Mg^{2+}[12]) cannot resist erosion from HF, they fail to considerably improve the electrochemical performance of cathodes. Consequently, crystal structures vary according to these effects[9]. Rare metal elements have been widely adopted due to their strong structural stability and chemical inertness. Therefore, compared to $xLi_2MnO_3 \cdot (1-x)LiMO_2$ (M = Mn, Ni, Co, etc.), rare earth elements will be one of the most competitive elements in studies on the doping modification of cathode materials. In addition, to improve doping, the ionic radius of the doping elements should be similar to those of Mn^{4+} (0.053 nm), Ni^{2+} (0.069 nm) and Co^{3+} (0.0685 nm). By referring to the periodic table of elements, Er^{3+} is the best-fitting metal ion for these experiments with an approximate ionic radius of 0.089 nm as a lanthanide.

In this research, through the combination of co-precipitation and a high-temperature sintering method, the original cathode material (0.6 $Li_2MnO_3 \cdot 0.4$ $LiMn_{1/3}$ $Ni_{1/3}Co_{1/3}O_2(Li_{1.20}Mn_{0.54}Ni_{0.13}Co_{0.13}O_2)$) and the material with Er^{3+} doping are prepared. Through the comparison of the cathode material properties (e.g., morphologies, microstructures and electrochemical properties) before and after Er^{3+} doping, the effects of Er^{3+} with different doping quantities are evaluated on the modification of $Li_{1.20}[Mn_{0.54}Ni_{0.13}Co0_{.13}]O_2$.

2. EXPERIMENTAL

2.1 Materials preparation

Carbonate precursor powders $[Mn_{0.54-x}Ni_{0.13}Co_{0.13}Er_x](Co_3)_{0.8}$ (x = 0, 0.01, 0.02, 0.03) were compounded through co-precipitation. The specific process was as follows: (1) the homogeneous mixing solution was prepared by dissolving and stirring $MnSO_4 \cdot H_2O$, $NiSO_4 \cdot 6H_2O$, $CoSO_4 \cdot 7H_2O$ and $Er(NO_3)_3 \cdot 6H_2O$ in a certain stoichiometric ratio; (2) $NH_3 \cdot H_2O$ and NaOH (the complexing agent and precipitant, respectively) solutions were added to the reaction kettle with continuous stirring. During the entire reaction, the pH of the solution was controlled at 8.0, the temperature was maintained at 60 ℃ and the stirring speed was kept at 800 r/min; (3) once the co-precipitation of the metal ions was complete, they were stirred for 12 h. Through filtering, washing and drying the acquired mixture, the power (i.e., $[Mn_{0.54-x}Ni_{0.13}Co_{0.13}Er_x] (CO_3)_{0.8}$ (x = 0, 0.01, 0.02, 0.03)) was obtained.

Then, in a stoichiometric ratio of 0.8:1.2, the precursor powder and $LiOH \cdot H_2O$ powder (exceeding 3 wt.%) were ground homogeneously, and subsequently, the mixture was pre-sintered in a tube furnace at 500 ℃ for 5 h. Finally, the cathode materials, $Li_{1.20}[Mn_{0.54-x}Ni_{0.13}Co_{0.13}Er_x]O_2$ (x = 0, 0.01, 0.02, 0.03) (i.e., Er^{3+} in doping quantities of 0, 0.01, 0.02 and 0.03, respectively), were acquired after sintering for 12 h at 950 ℃.

2.2 Materials characterization

The crystal structures were analyzed for the cathode materials before/after doping with Er^{3+} using a D8 Advance X-ray diffractometer (XRD, Bruker Corporation, Germany) under the following conditions: Cu target as the radiation source, voltage of 40 kV, current of 40 mA, step length of 0.02º, scanning speed of 2º/min and scanning range (2θ) of 10º~80º. Through scanning electron microscopy (SEM) with a JMS-7001 instrument, the morphologies and particle sizes of the 4 synthetic samples were observed. In addition, through inductively coupled plasma optical emission spectroscopy (ICP-OES) using an iCAP 6000 instrument, element composition analysis was performed for the 4 samples (e.g., $Li_{1.20}[Mn_{0.54-x}Ni_{0.13}Co_{0.13}Er_x]O_2$ (x = 0, 0.01, 0.02, 0.03)).

2.3 Electrochemical performance measurements

CR2025 button batteries were assembled from the cathode materials before/after Er^{3+} doping, and electrochemical performance measurements were conducted. Each battery consisted of the synthetic material as the cathode, lithium as the negative electrode, and a Celgard2300 polypropylene porous membrane as the diaphragm. The preparation process of the cathode was as follows: the cathode material powder was blended before/after evenly coating with SmF_3 (75 wt.%), the battery anode materials, conductive agent (i.e., Super P, 15 wt.%) and PVDF (10 wt.%), and then, a suitable amount of solvent (i.e., N-methyl pyrrolidone (NMP)) was added for size mixing. Then, the cathodes were evenly coated with aluminum foil with a thickness of 20 μm using the acquired slurry and drying the coating at 110 ℃ for 10 h under vacuum. The cathode was obtained by punching the coated foil into a wafer with a diameter of 12 mm by a tablet press. The above-mentioned positive electrode material, negative electrode material and diaphragm were put into a glove box containing N_2 for assembly. EC/DEC with a mass ratio of 1:1 dissolved in $LiPF_6$ (1 mol/L) was used as the electrolyte, which was injected into the CR2025 button batteries. Charge and discharge tests were carried out for all the assembled CR2025 button batteries using an LAND CT2001A battery tester under specific conditions (i.e., voltage between 2.0 V and 2.0 V, current intensity of 1 C = 250 mA g^{-1}, and test temperature of 25ºC). Utilizing a CHI660D electrochemical workshop, cyclic voltammetry was conducted with a scanning rate of 0.1 mV/s and scanning voltage from 2.0 to 4.8 V. Electrochemical AC impedance tests were performed for the CR2025 button batteries using the workshop with a signal amplitude of 5 mV and scanning frequency varying from 0.01 Hz to 100 kHz.

3. RESULTS AND DISCUSSION

Fig. 1 shows the XRD patterns of the $Li_{1.20}[Mn_{0.54}Ni_{0.13}Co_{0.13}]O_2$ cathode materials before/after Er^{3+} doping. XRD of all the samples showed sharp peaks and no impurity phases, which indicates that the materials have a classical layered α-NaFeO$_2$ structure in the R-3m space group. Weaker diffraction peaks lying between 20~25° corresponded to the arrangement (i.e., superlattice ordered structure composed of Li and Mn atoms) of $LiMn_6$ in intermediate metals, belonging to the monoclinic system in the C/2m space group[13,14]. The adjacent peaks (i.e., (006)/(012) and (018)/(110)) were well

divided, indicating that the synthetic cathode materials had integrated layered structures and excellent crystallinity[15]. In addition, similar to the XRD patterns of the original samples, other peaks were not detected in the XRD patterns of the samples with Er^{3+} doping, possibly attributing to the small doping quantity of Er^{3+}. Fig. 1 shows the lattice structure parameters of the $Li_{1.20}[Mn_{0.54}Ni_{0.13}Co_{0.13}]O_2$ cathode materials before/after Er^{3+} doping and the intensity ratios of the (003) and (104) diffraction peaks. The intensity ratio, I(003)/I(104) (R), is related to the cationic mixing degree of the layered crystalline materials. Especially, when R > 1.2, it shows that the mixing degree between Li^+ and Ni^{2+} was lower in the cathode material[16, 17]. As seen from the table, as the doping quantity of Er^{3+} increased gradually, the R values for the 4 samples were 1.51, 1.68, 1.76 and 1.72 ((x = 0, 0.01, 0.02, and 0.03, respectively). This illustrates that Er^{3+} doping can effectively inhibit cation mixing of the cathode materials. In addition, the lattice constant ratio c/a depended on the layered structural stability of the cathode materials, and the constant ratios of the 4 samples were all over 4.90. Therefore, this indicates that the synthetic materials had perfect layered structural stability[18].
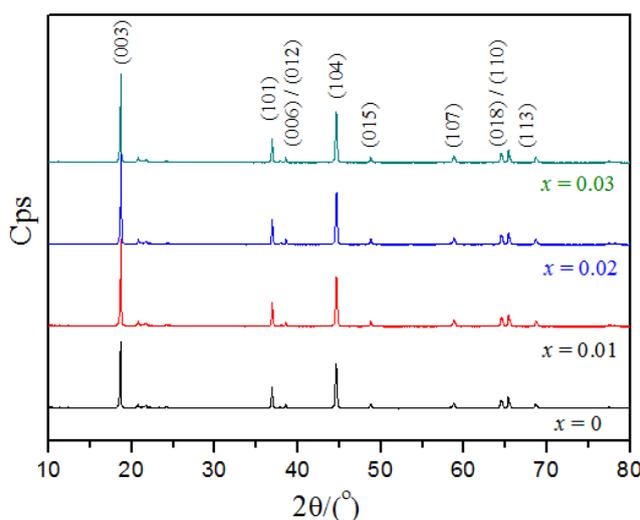

Figure 1. XRD spectra of $Li_{1.20}[Mn_{0.54-x}Ni_{0.13}Co_{0.13}Er_x]O_2$(x = 0, 0.01, 0.02, 0.03).

Table 1. Lattice parameters and intensity ratios of $Li_{1.20}[Mn_{0.54-x}Ni_{0.13}Co_{0.13}Er_x]O_2$(x = 0, 0.01, 0.02, 0.03).

x	a (Å)	c (Å)	c/a	$R=I_{(003)}/I_{(104)}$
0	2.8522	14.2206	4.9858	1.51
0.01	2.8528	14.2283	4.9875	1.68
0.02	2.8531	14.2384	4.9905	1.76
0.03	2.8553	14.2447	4.9890	1.72

Fig. 2 shows the SEM images of the $Li_{1.20}[Mn_{0.54}Ni_{0.13}Co_{0.13}]O_2$ cathode materials before/after Er^{3+} doping. As seen from the figure, all the samples consisted of particles with sizes between 300 nm and 500 nm and rocky structures. This indicates that Er^{3+} doping did not cause an obvious transformation to the morphology. With an increasing doping quantity of Er^{3+}, the particle size increased continuously, showing that Er^{+3} doping can enhance the crystallinity of the cathode material.

These experimental results will help refine the electrochemical performances of the cathode materials. Table 2 presents the elemental content analysis of the $Li_{1.20}[Mn_{0.54-x}Ni_{0.13}Co_{0.13}Er_x]O_2$ (x = 0, 0.01, 0.02, 0.03) cathode materials. According to the data in the table, the elemental contents (i.e., Mn, Ni, Co and Er contents) in the $Li[Li_{0.2}Mn_{0.54}Ni_{0.13}Co_{0.13}]O_2$ synthetic cathode materials with various Er^{3+} doping quantities were approximately equal to designed experimental values. Therefore, the synthetic samples achieve the desired requirements.
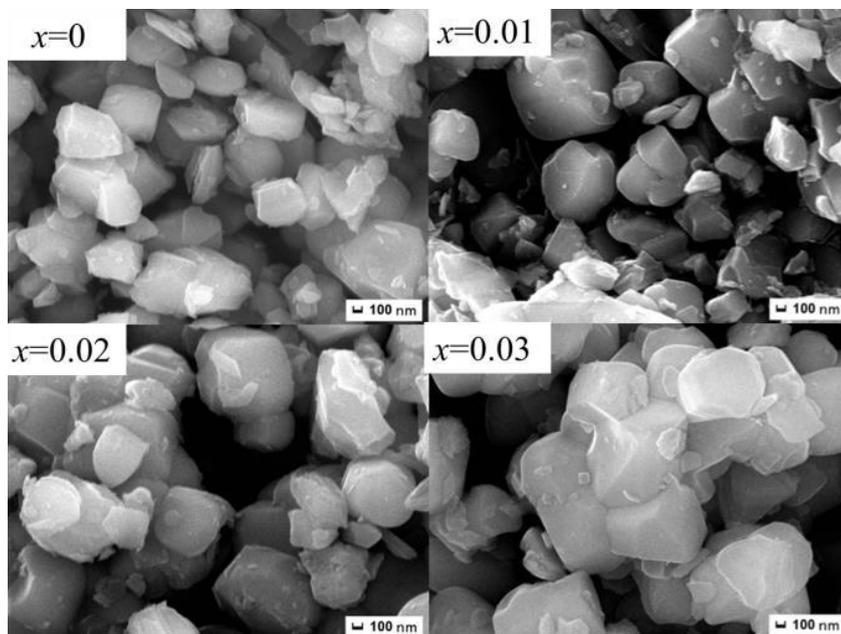

Figure 2. SEM images of $Li_{1.20}[Mn_{0.54-x}Ni_{0.13}Co_{0.13}Er_x]O_2$ (x = 0, 0.01, 0.02, 0.03).

Fig. 3 shows the initial charge and discharge curves of the $Li_{1.20}[Mn_{0.54}Ni_{0.13}Co_{0.13}]O_2$ cathode materials before/after Er^{3+} doping at a rate of 0.1 C and voltage from 2.0 to 4.8 V. During initial charging, the charge curves for all the samples were characterized by two parts: (1) a rising area with the voltage gradually increasing from 2.0 V to 4.5 V. Li^+ could escape from the main phase (i.e., $LiMn_{1/3}Ni_{1/3}Co_{1/3}O_2$) with the oxidization of Ni^{2+} and Co^{3+} to Ni^{4+} and Co^{4+}. (2) The voltage plateau area at a voltage of 4.5 V. During charging, Li^+ was oxidized to Li_2O, escaping from Li_2MnO_3 irreversibly. This resulted in an initial irreversible capacity loss[19, 20]. With an increase of the Er^{3+} doping quantity, the discharge specific capacity of the 3 samples after doping (x = 0.01, 0.02, 0.03) were 261.3, 271.5 and 267.0 mAh g^{-1}, respectively, while that of the sample without doping was only 254.2 mAh g^{-1}. In addition, the initial coulomb efficiency of the $[Mn_{0.54}Ni_{0.13}Co_{0.13}]O_2$ cathode material was improved by doping. The initial coulomb efficiencies of the 4 samples (x = 0.01, 0.02, 0.03) were 72.0%, 74.6%, 78.9% and 74.8%, respectively. This mainly resulted from the excellent crystallinity, which improved the electrochemical properties of the materials. Therefore, the irreversible capacity loss was reduced, and the initial discharge specific capacity increased. After the traditional method of Al^{3+} doping in $Li[Li_{0.2}Mn_{0.54}Ni_{0.13}Co_{0.13}]O_2$ to improve the performance, the initial Coulomb efficiency was increased to 76%, slightly lower than that achieved by Er^{3+} doping[21].

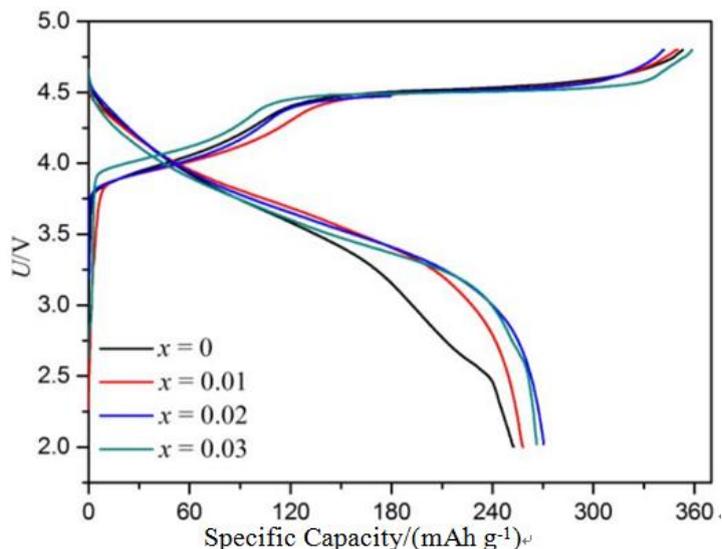**Figure 3.** Initial charge and discharge curves of $Li_{1.20}[Mn_{0.54}Ni_{0.13}Co_{0.13}]O_2$ (x = 0, 0.01, 0.02, 0.03)
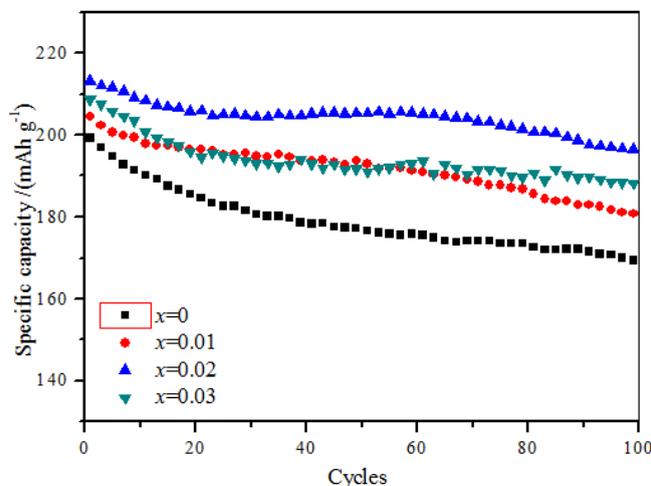

Figure 4. Cycle performances of $Li_{1.20}[Mn_{0.54}Ni_{0.13}Co_{0.13}]O_2$(x = 0, 0.01, 0.02, 0.03).

Fig. 4 presents the performances over 100 cycles of the $Li_{1.20}[Mn_{0.54}Ni_{0.13}Co_{0.13}]O_2$ cathode materials before/after Er^{3+} doping at a rate of 0.5 C and voltage from 2.0~4.8 V. Evidently, the cycle performances of the samples with Er^{3+} doping were superior to that of the original sample. When the doping quantity of Er^{3+} was 0.02, the cycle performance of $Li_{1.20}[Mn_{0.52}Ni_{0.13}Co_{0.13}Er_{0.02}]O_2$ was optimum. As the doping quantity of Er^{3+} increased, the initial discharge specific capacities of the 4 samples were 199.7, 204.9, 212.5 and 209.1 mAh g^{-1} (x = 0, 0.01, 0.02, 0.03, respectively). After 100 cycles, the discharge specific capacity decreased to 169.0, 180.5, 197.1 and 188.6 mAh g^{-1}, respectively, and the corresponding capacity retention ratio increased from 84.6% to 88.1% to 92.8% and then subsequently decreased to 90.2%. The excellent cycle performances of the samples after Er^{3+} doping were mainly attributed to the Er^{3+} doping modification reducing cation mixing in the cathode materials, thus enhancing the layered structural stability of the materials. Therefore, the stability of cathode was promoted. However, after 40 cycles, the capacity retention ratio of

$Li[Li_{0.2}Mn_{0.51}Sm_{0.03}Co_{0.13}Ni_{0.13}]O_2$ was 82.12% [22]. With modification by Y^{3+} doping, the first discharge specific capacity of $Li[Li_{0.20}Mn_{0.534}Ni_{0.133}Co_{0.133}]O_2$ at a rate of 0.1 C was 349.7 mAh g^{-1}. After 80 cycles, the discharge capacity decreased to 225.2 mAh g^{-1}, and the capacity retention rate was only 64.4% [9].

Regarding electric vehicles and hybrid electric vehicles, the rate capability of the battery is a key performance aspect to consider. Fig. 5 describes the rate capabilities of the $Li_{1.2}Mn_{0.54}Ni_{0.13}Co_{0.13}O_2$ cathode materials before/after Er^{3+} doping with various specific rates (i.e., 0.1 C, 0.2 C,0.5 C, 1 C, 2 C and 5 C) and voltages (i.e., 2.0~4.8 V). As seen from Fig. 5, the discharge specific capacities of the samples with Er^{3+} doping under different rates were considerably higher than that of the sample without doping. As the doping quantity of Er^{3+} increased, the rate capability of the 4 samples increased initially and subsequently decreased. Particularly, when the quantity was 0.02, the $Li_{1.20}[Mn_{0.52}Ni_{0.13}Co_{0.13}Er_{0.02}]O_2$ sample performed optimally with the best rate capability. As the current density of the battery increased to 5 C, the discharge specific capacity of $Li_{1.20}[Mn_{0.52}Ni_{0.13}Co_{0.13}Er_{0.02}]O_2$ increased to 117.6 mAh g^{-1}, higher than 94.6 mAh g^{-1} of the sample without doping. With Er^{3+} doping, the lattice constant of the unit cell was expanded, and during battery cycling, Li^+ could migrate conveniently under a smaller confinement or escaping resistance. Therefore, the samples with Er^{3+} doping had superior rate capabilities. When the material discharged at 0.1 C the second time, the capacity retention ratios of the samples with Er^{3+} doping were higher than those in the first discharge at 0.1 C. The discharge specific capacity of the original sample without doping decreased by 20 mAh g^{-1}, and the reversible capacity accounted for 92.0%. These results reveal that the reversible escaping and embedding of Li^+ benefited from Er^{3+} doping in the cathode materials. With modification by Y^{3+} doping of the $Li[Li_{0.20}Mn_{0.534}Ni_{0.133}Co_{0.133}]O_2$ cathode materials, the discharge specific capacity at a rate of 0.1 C was only 116.1 mAh g^{-1}, which was close to the value of the discharge specific capacity at a rate of 5 C in this paper [9].
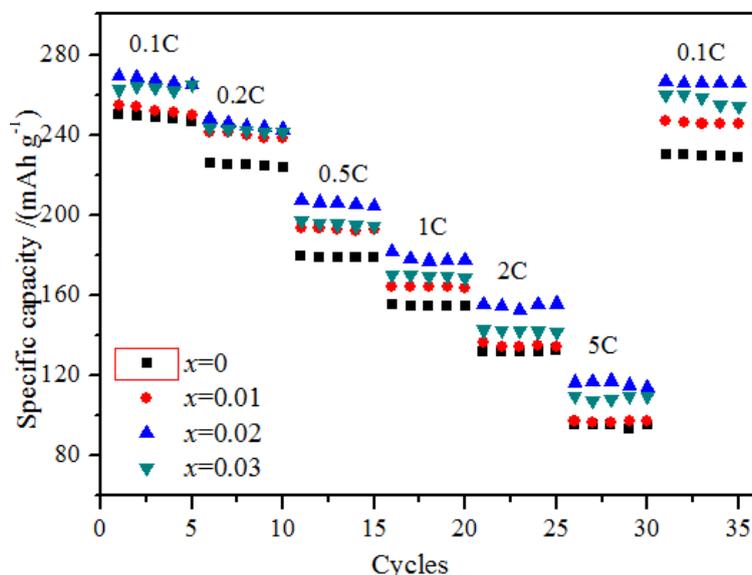

Figure 5. Rate capacities of $Li_{1.20}[Mn_{0.54}Ni_{0.13}Co_{0.13}]O_2$ (x = 0, 0.01, 0.02, 0.03).

4. CONCLUSIONS

Using co-precipitation, carbonate precursors (i.e., $[Mn_{0.54-x}Ni_{0.13}Co_{0.13}Er_x](CO_3)0.8$ (x = 0, 0.01, 0.02, 0.03)) were prepared. Upon sintering the carbonate precursors and $LiOH \cdot H_2O$ at a high temperature, cathode materials (i.e., $Li_{1.20}[Mn_{0.54-x}Ni_{0.13}Co_{0.13}Er_x]O_2$ (x = 0.01, 0.02, 0.03)) were produced. SEM, XRD and ICP-OES results revealed that Er^{3+} doping improved the crystallinity and reduced cation mixing in the lattice of $Li_{1.20}[Mn_{0.54-x}\ Ni_{0.13}\ Co_{0.13}\ Er_x]O_2$ (x = 0.01, 0.02, 0.03). Compared to the original sample (i.e., $Li_{1.20}[Mn_{0.54}Ni_{0.13}Co_{0.13}]$) without Er^{3+} doping, the doped cathode materials (i.e., $Li_{1.20}[Mn_{0.54-x}Ni_{0.13}Co_{0.13}Er_x]O_2$ (x = 0.01, 0.02, 0.03)) displayed superior performances with smaller losses of the initial irreversible capacity, more stable cycle performances and excellent rate capacities. After 100 cycles, the discharge specific capacity of $Li_{1.20}[Mn_{0.52}Ni_{0.13}Co_{0.13}Er_{0.02}]O_2$ was 197.1 mAh g^{-1}, and the capacity retention ratio remained 92.8%, while 84.6% of the capacity was maintained in the sample (i.e., $Li_{1.20}[Mn_{0.54}Ni_{0.13}Co_{0.13}]O_2$) without Er^{3+} doping.

References

1. L.H. Xu, Q.F. Huang, C. Su, X.G. Zhu, and C. Zhang, *J. Nanosci. Nanotechnol*, 16(2016) 588.
2. Z. Yi, *J Mater Sci: Mater Electron*, 27(2016) 10347.
3. F. Wu, Z. WANG,and Y. F. Su, *Journal of Power Sources*, 247(2014) 20.
4. C. D. Li, J. Xu, J. S. Xia, *Solid State Ionics*, 292(2016)75.
5. S. Sun, N. Wan, Q. Wu, X. Zhang, D. Pan, Y. Bai, X. Lu, *Solid State Ionics*, 278(2015) 85.
6. B. H. Song, M. O. Lai, L. Lu. *Electrochimica Acta*, 80(2012)187.
7. S. J. Han, B. Qiu, Z. Wei, *Journal of Power Sources*, 268(2014) 683.
8. S. H. Kang，M. M. Thackeray, *Journal of The Electrochemical Society*, 155(2008)269.
9. S. F. Kang, H. F. Qin, Y. Fang, *Electrochimica Acta*, 144(2014) 22.
10. J. M. Zheng, X. B. Wu, and Y. Yang, *Electrochimica Acta*, 105(2013) 200.
11. F. Lian, M. Gao, W. H. Qiu, *Journal of Applied Electrochemistry*, 42(2012) 409.
12. X. Jin, Q. J. Xu, H. M. Liu, *Electrochimica Acta*,136(2014) 19.
13. J. Y. Du, Z. Q. Shan, K. L. Zhu, *J Solid State Electrochem*, 19(2015) 1037.
14. S. J. Shi, J. P. Tu, Y. J. Zhang, *Electrochemica Acta*, 108(2013) 441.
15. W. Yuan, H. Z. Zhang, Q. Liu, *Electrochimica Acta*, 135(2014) 199.
16. C. Lu, H. Wu, Y. Zhang, *Journal of Power Sources*, 267(2014) 682.
17. Z. Y. Wang, E. Z. Liu, C. N. He, *Journal of Power Sources,* 236(2013) 25.
18. S. W. Cho, G. O. Kim, K. S. Ryu, *Solid State Ionics*, 206(2012) 84.
19. D. Q. Liao, C. Y. Xia, X. M. Xi, *J Sol-Gel Sci Technol*, 78(2016) 403
20. G. F, Xu, J. L. Li, Q. R. Xue, *Journal of Power Sources*, 248(2014) 894.
21. J. Charl, I. Kenneth, *Electrochimica Acta*, 85(2012) 411.
22. G. F. Xu, Q. R. Xue, J. L. Li, *Solid State Ionics*, 293(2016) 7.